

Optimal Design of Coatings for Mirrors of Gravitational Wave Detectors: Analytic *Turbo* Solution via Herpin Equivalent Layers

Vincenzo Pierro,^{1,2} Vincenzo Fiumara,^{3,2} and Francesco Chiadini^{4,2}

¹*Dipartimento di Ingegneria (DING), Università del Sannio, I-82100 Benevento, Italy.*

²*INFN, Sezione di Napoli Gruppo Collegato di Salerno,*

*Complesso Universitario di Monte S. Angelo, I-80126 Napoli, Italy.**

³*Scuola di Ingegneria, Università della Basilicata, I-85100 Potenza, Italy.*

⁴*Dipartimento di Ingegneria Industriale, DIIN, Università di Salerno, I-84084 Fisciano, Salerno, Italy*

In this paper, an analytical solution to the problem of optimal dielectric coating design of mirrors for gravitational wave detectors is found. The technique used to solve this problem is based on Herpin's equivalent layers, which provide a simple, constructive, and analytical solution. The performance of the Herpin-type design exceeds that of the periodic design and is almost equal to the performance of the numerical, non-constructive optimized design obtained by *brute force*. Note that the existence of explicit analytic constructive solutions of a constrained optimization problem is not guaranteed in general, when such a solution is found, we speak of *turbo* optimal solutions.

Keywords: Dielectric multilayers; Gravitational Wave Interferometric Detectors; Coating Optimization

I. INTRODUCTION

The development of optimized coatings for the end test-masses of the gravitational wave interferometers is one of the important goals to be achieved for improving the sensitivities of gravitational wave detectors [1, 2]. Indeed, the coating Brownian noise is the most relevant source of noise in the band of interest for astrophysical observation. To reduce this source of noise, researchers can act by using different materials with the best properties for the mirrors, optimizing the interferometer's laser beam, lowering the temperature to cryogenic values, and finally acting on the coating design. Unfortunately, there are not many glassy materials that satisfy the optical requirements necessary for gravitational wave detectors, the improvement of the laser beam would require a rethinking of the whole interferometer cavity as well as make this cavity cryogenic (see the papers [3–5] for a review on the subject).

In this work, we explore the possibility of optimizing the design of the mirrors by acting on the thicknesses of the layers that form the coating, with the materials currently available. Although coatings made of multiple materials [6–8] (obtained, in some cases, from cascades of binary designs) have been recently proposed, further study of binary coating theory provides the theoretical tools to understand more complex approaches.

It is well known [9] that the electrodynamics of multilayers structures, like those depicted in Figure 1, can be described in a semi-analytic way with the method of the characteristic matrices of the layers (also called transmission matrices [10]). The characteristic matrix of the m -th layer can be written [11, 12]:

$$\mathbf{T}_m = \begin{bmatrix} \cos(\psi_m) & i(n^{(m)})^{-1} \sin(\psi_m) \\ in^{(m)} \sin(\psi_m) & \cos(\psi_m) \end{bmatrix}, \quad (1)$$

where $\psi_m = \frac{2\pi}{\lambda_0} n^{(m)} d_m$ is the electric phase, λ_0 and d_m are the free space wavelength and the layer thickness, respectively, and $n^{(m)} = n_r^{(m)} - i\kappa^{(m)}$ is the complex refractive index. Here $\kappa^{(m)}$ is the extinction coefficient, which for the considered materials will be negligible (i.e., $\kappa^{(m)} \sim 10^{-8}$).

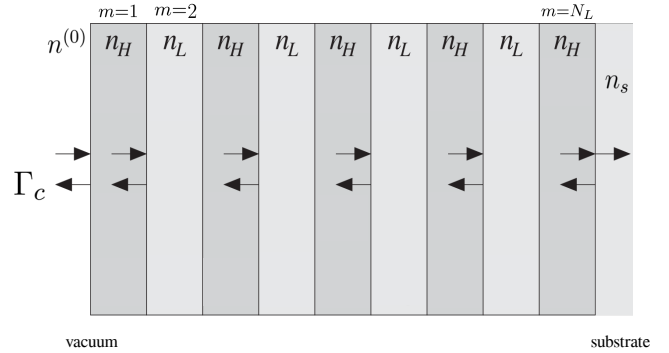


FIG. 1. In the figure an example of binary coating made of alternating L and H type materials is displayed. The laser light is normally incident from the left (i.e., a monochromatic wave, an $\exp i\omega t$ dependence on time is supposed), Γ_c is the reflection coefficient of the stratified medium. The refractive index of the m -th layer is in general $n^{(m)}$, for binary coating the sequence of refractive index is alternating with values n_H (high refractive index) and n_L (low refractive index). The substrate refractive index is n_s , the leftmost half space has, refractive index $n^{(0)}$ (here it is supposed to be the vacuum).

The optical response of the whole coating (i.e., the transmittance) can be computed from the multilayer characteristic matrix,

$$\mathbf{T} = \mathbf{T}_1 \cdot \mathbf{T}_1 \cdot \dots \cdot \mathbf{T}_{N_L} \quad (2)$$

where N_L is the total number of layers numbered from the vacuum to the substrate as illustrated in Figure 1. To write Equation (2) we use the property that the characteristic matrix of a sequence of layers is the product of the characteristic matrices of the individual layers.

The transmittance calculation is done in two steps, first

* corresponding: pierro@unisannio.it, vpierro@sa.infn.it

the equivalent reflection index n_c of the multi-layer structure, and then the reflection coefficient Γ_c at the vacuum interface are computed. The complex reflection coefficient Γ_c at the vacuum/coating interface is given by:

$$\Gamma_c = \frac{n^{(0)} - n_c}{n^{(0)} + n_c} \quad (3)$$

where n_c is the effective refractive index of the whole multilayer structure,

$$n_c = \frac{T_{21} + n_s T_{22}}{T_{11} + n_s T_{12}}. \quad (4)$$

The power transmittance at the vacuum/coating interface is $\tau_c = 1 - |\Gamma_c|^2$. In the case of binary coating we have:

$$\begin{cases} n^{(m)} = n_H - \kappa_H, & m \text{ odd}, & n^{(m)} = n_L - \kappa_L, & m \text{ even}; \\ \phi_m = \phi_H, & m \text{ odd}, & \phi_m = \phi_L, & m \text{ even}; \\ Y_m = Y_H, & m \text{ odd}, & Y_m = Y_L, & m \text{ even}. \end{cases} \quad (5)$$

These multilayer structures are made of N_L alternating high n_H and low n_L refractive indexes deposited on a substrate of refractive index n_s . The coefficients ϕ_H and ϕ_L are the mechanical losses and Y_H and Y_L are the Young moduli of the two materials. Let us also introduce the specific noise coefficients that will be used in the following:

$$\eta_L = \frac{1}{\sqrt{\pi}w} \phi_L \left(\frac{Y_L}{Y_s} + \frac{Y_s}{Y_L} \right) \quad \eta_H = \frac{1}{\sqrt{\pi}w} \phi_H \left(\frac{Y_H}{Y_s} + \frac{Y_s}{Y_H} \right), \quad (6)$$

where w is the (assumed Gaussian) laser-beam waist. Thermal noise in gravitational detectors is the most important limitation for their operation. We refer the reader to the works in [13–15] for an exhaustive description of the problem and the proposed solutions [16, 17] in the operating observatory Virgo [1] and LIGO [2].

A straightforward formulation of the coating optimization problem for the design of low noise dielectric mirror can be:

$$\begin{aligned} & \text{Minimize}_{z_1, \dots, z_{N_L} \in \Omega} \quad \bar{\phi}_c \\ & \text{subject to} \quad \tau_c \leq \tau_0 \end{aligned} \quad (7)$$

where the constraint transmittance τ_0 should be a few parts per million (ppm), typically $\tau_0 = 6$ ppm.

Defining the normalized loss angle $\bar{\phi}_c = \phi_c / (\lambda_0 \eta_L)$ and introducing the normalized physical length $z_m = d_m / \lambda_0$, where λ_0 is the free-space wavelength of the laser, we have for binary coatings:

$$\bar{\phi}_c = {}^o\Sigma_{m=1}^{N_L} \gamma z_m + {}^e\Sigma_{m=1}^{N_L} z_m, \quad (8)$$

where summation ${}^e\Sigma$ (resp. ${}^o\Sigma$) is on the even (resp. odd) integer such that $1 \leq m \leq N_L$. The noise ratio coefficient in Equation (8), i.e., $\gamma = \eta_H / \eta_L$, can be explicitly written for binary coating as:

$$\gamma = \frac{\phi_H}{\phi_L} \left(\frac{Y_H}{Y_s} + \frac{Y_s}{Y_H} \right) \left(\frac{Y_L}{Y_s} + \frac{Y_s}{Y_L} \right)^{-1}. \quad (9)$$

In the case where the refractive index n_L is the same as that n_s of the substrate material (as in current gravitational wave detectors) N_L is an odd number. The choice of an even N_L would lead to a configuration with the rightmost layer (near the substrate) made of low refractive index material (the same as the substrate) that would increase noise without having any effect on reflectivity. The search space Ω is defined by the inequalities $0 \leq z_m \leq 0.25/n_H$ for odd m and $0 \leq z_m \leq 0.5/n_L$ for even m . An alternative and equivalent way to formulate the optimization problem (as shown in [18]) is

$$\begin{aligned} & \text{Minimize}_{z_1, \dots, z_{N_L} \in \Omega} \quad \tau_c \\ & \text{subject to} \quad \bar{\phi}_c \leq \bar{\phi}_0 \end{aligned} \quad (10)$$

where $\bar{\phi}_0$ is a prescribed maximum allowed loss angle.

II. THE HERPIN EQUIVALENT LAYER OPTIMIZATION PROBLEM

According to Herpin's equivalent layer theorem [19] a symmetrical multilayer stack (i.e., a *palindrome* sequence of dielectric thin films) is equivalent to a single layer. This theorem is based on the fact that the two elements on the main diagonal of the characteristic matrix of any palindromic sequence of materials are equal.

In this paper, we consider an equivalent Herpin layer that consists of three physical layers arranged in an *LHL*-type sequence. According to the general theorem, this sequence must be dielectrically and geometrically symmetric, so both materials and layer thicknesses must be palindromic. Thus denoting by p and q the normalized lengths of the layers L and H respectively, below are shown, using a simple computation, the relevant elements of the transmission matrix $\mathbf{T}^{(E)}$ of the considered *virtual layer* $E = LHL$:

$$T_{11}^{(E)} = \cos(2\pi q n_H) \cos(4\pi p n_L) - \frac{(n_H^2 + n_L^2) \sin(2\pi q n_H) \sin(4\pi p n_L)}{2n_H n_L}, \quad (11)$$

$$T_{12}^{(E)} = i \left(-\frac{n_H \sin(2\pi q n_H) \sin^2(2\pi p n_L)}{n_L^2} + \frac{\sin(2\pi q n_H) \cos^2(2\pi p n_L)}{n_H} + \frac{\cos(2\pi q n_H) \sin(4\pi p n_L)}{n_L} \right). \quad (12)$$

It can be verified by inspection, and this is also the main result of Herpin's theorem, that $T_{11}^{(E)} = T_{22}^{(E)}$, and because of the unitary constraint on the determinant of the characteristic matrix T , the last element is uniquely determined by solving the following equation w.r.t. $T_{21}^{(E)}$:

$$(T_{11}^{(E)})^2 - T_{12}^{(E)} T_{21}^{(E)} = 1. \quad (13)$$

To understand the reasons that lead to formulating the present analytical solution, we summarize the results of the papers [18, 20]. In the paper [18], a multi-objective optimization (with the BorgMOEA algorithm [21]) without *a priori* hypothesis was applied to the problem of general optimization of binary coatings for gravitational wave detectors mirrors.

It has been shown in [18] that the Pareto front remains the same whether one sets up a code that solves problem (7) or implements problem (10), so the two formulations considered are equivalent. Moreover, in the same paper we show that the optimal design is made by the following sequences of layers $L(HL)^{N_D}H$. The sequence of thicknesses associated with this solution is given by $z_{L,i}(z_H z_L)^{N_D} z_{H,f}$, where in general $z_{L,i} \neq z_L$, $z_{H,f} \neq z_H$. This solution is periodic except for the first and last layers, and that is why the solution has been called periodic with initial and final tweaking. Furthermore z_L , z_H satisfy an approximate Bragg condition $n_L z_L + n_H z_H \sim 0.5$.

In the paper [20], a very simple periodic solution $(HL)^{N_D}H$ was studied and experimentally validated [22]. In these articles the tweaking procedure has been considered but only as a possible second step of improvement of the periodic design, considering the thicknesses of the innermost layers fixed to the values calculated in the first step. This solution approximates that which would be found by optimizing on all four layers simultaneously, that is implemented in [18].

Finally, in the paper [18] (see Equation (20) therein) it

has been shown that the Pareto front of the optimized solutions is placed close to the transmittance versus thermal noise line relative to a suitable (virtual) quarter-wave design.

So far, we have mentioned almost exhaustively all the existing literature on the coating optimization problem. For the sake of completeness, although not completely relevant, let us mention [23] which proposes a physical-mathematical approach to the computation of the best periodic design, we emphasize that the method is not based on solving an optimization problem.

Taking into account the hints introduced above, we assume that the optimal solution is of the form $(EL)^{N_D}E$ where E is an equivalent Herpin layer, as introduced above, and L is a quarter-wave layer. We note that in these designs the last layer is of type E , i.e., it is a *virtual layer* consisting of an LHL sequence. Additionally, in this case, the last physical layer (near the substrate) of type L in the last *virtual layer* E is not considered because it is made of the same material as the substrate and does not contribute to the dielectric contrast (actually, the last interface does not exist, it is fictitious).

We are now able, from all these ansatz introduced above, to reformulate the optimization problem as follows:

$$\begin{aligned} & \text{Minimize}_{p,q,N_D} \quad \bar{\phi}_c \\ & \text{subject to} \quad E \in QWL \text{ and } \tau_c \leq \tau_0 \end{aligned} \quad (14)$$

here QWL is the set of quarter wavelength transmission matrix and $\bar{\phi}_c$ is determined by the normalized physical length p , and q . We have

$$\bar{\phi}_c = (N_D + 1)\gamma q + (2N_D + 1)p + N_D p_{1/4}, \quad (15)$$

where $p_{1/4} = 1/(4n_L)$ is the normalized quarter wavelength thickness of L layer. The condition $E \in QWL$ can be explicated by requiring $T_{11}^{(E)} = 0$ i.e.,

$$\cos(2\pi q n_H) \cos(4\pi p n_L) - \frac{(n_H^2 + n_L^2) \sin(2\pi q n_H) \sin(4\pi p n_L)}{2n_H n_L} = 0. \quad (16)$$

III. NUMERICAL RESULTS

In this section, we compute the Pareto front of the three competing designs, i.e., the proposed design method in Equation (14), the periodic design [20] and the fully (*brute force*) optimized design [18]. Table I is used as a reference for the physical parameters of the L and H materials.

In Figure 2a the Pareto front $\mathcal{P}_H(\bar{\phi}_c)$ of the problem

(14) where $N_D \leq 15$ is shown in red on a log-linear scale as a function of the dimensionless quantity $\bar{\phi}_c$. The continuous black curve represents the Pareto front again for problem (14) but with $N_D = 10$ kept fixed. Finally, for fixed $N_D = 10$ the dashed curves show the Pareto front of the optimal periodic doublet design. 0

In Figure 2b, a close-up of the central area of the Figure 2a is shown along with several Pareto fronts of Herpin (continuous curves) and periodic (dashed curves) designs.

Coating	Substrate
H (amorphous Ti-doped Ta_2O_5)	(bulk crystalline SiO_2)
L (SiO_2)	
$n_H = 2.10$	$n_s = 1.45$
$n_L = 1.45$	$Y_s = 72$ GPa
$\kappa_H = 4.0 \times 10^{-8}$	$\kappa_s = 8.4 \times 10^{-11}$
$\kappa_L = 8.4 \times 10^{-11}$	$\phi_s = 7.00 \times 10^{-8}$
$Y_H = 147$ GPa	
$Y_L = 72$ GPa	
$\phi_H = 3.76 \times 10^{-4}$	
$\phi_L = 5.00 \times 10^{-5}$	
$\gamma = 9.5$	

TABLE I. Physical parameters of coating and substrate material used in the simulations, we assume that the temperature is $T = 300$ K and free-space wavelength is $\lambda_0 = 1064$ nm. The two materials described above are those that have the best characteristics, mainly in terms of negligible extinction coefficients, and are used in both the Virgo [1] and LIGO [2] experiments.

From the analysis of Figure 2, it is clear that Herpin's design generates a Pareto front that consists of several bumps (a bumpy curve). This behavior had already been observed in the *brute force* solution given by the BorgMOEA method used in the paper [18]. This figure reveals that the various bumps of the complete Pareto front are parts of the Pareto curves with fixed N_D that intersect each other (see Figure 2b).

Moreover, as will be more evident later, we note that the periodic designs are always worse than Herpin's. Let us take a closer look at this result in Figure 3 to better illustrate it. The Pareto front of the periodic synthesis of the doublet (respectively of the BorgMoea) will be called with $\mathcal{P}_D(\bar{\phi}_c)$ (respectively with $\mathcal{P}_B(\bar{\phi}_c)$).

In Figure 3 the following normalized differences

$$\mathcal{D}_{DH} = \mathcal{P}_H(\bar{\phi}_c)^{-1}[\mathcal{P}_D(\bar{\phi}_c) - \mathcal{P}_H(\bar{\phi}_c)],$$

$$\mathcal{D}_{HB} = \mathcal{P}_H(\bar{\phi}_c)^{-1}[\mathcal{P}_H(\bar{\phi}_c) - \mathcal{P}_B(\bar{\phi}_c)], \quad (17)$$

are displayed. To be precise, in Figure 3 the function \mathcal{D}_{DH} is the dashed curve while \mathcal{D}_{HB} is the continuous black one. By inspection of the figure, it is clear that both the two normalized differences are *positive* and have discontinuity points in the cusps that separate the different bumps in the Pareto front curves. The value of these functions remains limited (about 3% for \mathcal{D}_{DH} and about 0.9% for \mathcal{D}_{HB}) even in the region with the highest noise (i.e., low transmittance), which is that of interest for gravitational applications.

In this connection, the values of the normalized thermal noise (on the Pareto front) for the three analyzed methods are reported in Table II for fixed values of the transmittance constraint. Some values of the transmittance constraint are shown in the first column of Table II together with the value of N_D giving the optimal solutions for all the three analyzed design methods, i.e., periodic doublets, *brute force* BorgMOEA and Herpin design. The values of the computed minimum normalized thermal noise $\bar{\phi}_c$ are reported in the other columns of the Table.

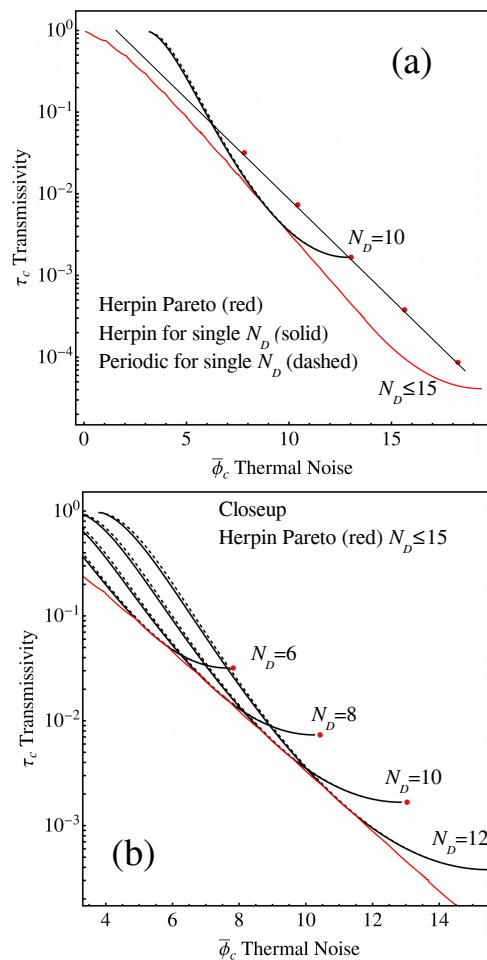


FIG. 2. The figure shows in (a), in red, the Pareto front by Herpin's method $\mathcal{P}_H(\bar{\phi}_c)$ obtained by keeping $N_D \leq 15$ as a function of dimensionless normalized mechanical loss $\bar{\phi}_c$. For fixed $N_D = 10$ the Herpin Pareto front (solid black) and the periodic Pareto front (dashed black) are displayed for comparison. Below in (b) a closeup of the central part of (a) where some additional fixed N_D Pareto curves has been displayed. The red dots in (a,b) are the quarter-wavelength designs for $N_D = 6, 8, 10, 12$.

This table confirms the results of Figure 3, i.e., even in the zone of very low transmittance, the Herpin-like semi-analytic method is the one that comes closest to the minimum value obtained with *brute force*, for which there is no simple constructive recipe.

IV. CONCLUSIONS

The production and characterization of layered systems with dimensions of hundreds of nanometers or less, to be used as highly reflective surfaces [24, 25] is a problem of great interest for improving the operation of gravitational wave antennas [1, 2]. Herpin's theorem allows obtaining an equivalent stratified material, consisting of three layers arranged in a *palindrome* sequence, which mimic exactly a quarter-wave layer. In this paper, these quarter-

Parameters	$\bar{\phi}_c$ Periodic doublet	$\bar{\phi}_c$ Borg MOEA	$\bar{\phi}_c$ Herpin
$N_D = 21$ $\tau_c = 6 \times 10^{-6}$	19.597	19.560	19.573
$N_D = 20$ $\tau_c = 1 \times 10^{-5}$	18.826	18.786	18.803
$N_D = 17$ $\tau_c = 6 \times 10^{-5}$	16.115	16.076	16.091
$N_D = 17$ $\tau_c = 1 \times 10^{-4}$	15.345	15.300	15.317

TABLE II. The table shows the normalized mechanical loss $\bar{\phi}_c$ for fixed transmittance for three different designs. The target transmittance τ_c and the number of layers N_D are reported in the first column. For these parameters, the minimal loss angles, obtained with the doublet, BorgMOEA, and Herpin procedures are displayed in the other columns.

wave equivalent layers are used in conjunction with normal (quarter-wave) layers made of low refractive index material, to produce optimized designs of coatings. The method reduces to an optimization problem with two independent parameters, namely the number of equivalent layers N_D and the normalized thickness of one of the materials defining the equivalent layer. Thus, a *turbo* solution to the problem (i.e., an explicit analytic constructive solution) can be found in a very simple way. Such a solution is closer to that obtained with the BorgMOEA method [18] than the doublet periodic one [20]. The prediction made in a previous article [18], namely that the BorgMOEA *brute force* design should be close to a virtual quarter-wave design, is fully confirmed. Indeed, in this paper, an explicit semi-analytic quarter-wave design is found, even of simple physical interpretation. The limi-

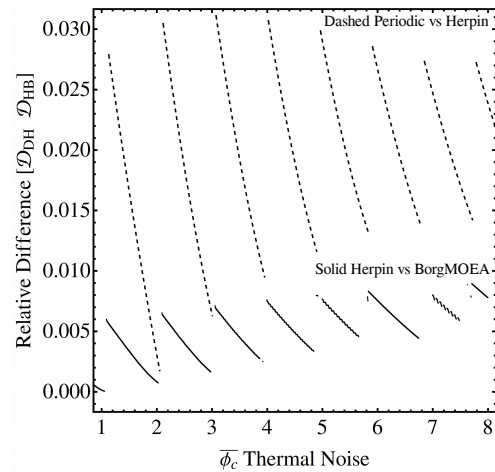


FIG. 3. In the figure the relative differences \mathcal{D}_{DH} (dashed) and \mathcal{D}_{HB} (solid) are displayed as a function of the dimensionless normalized mechanical loss $\bar{\phi}_c$. The performances of Herpin design exceed the performance of periodic design and are very close to the performances of *brute force* BorgMOEA numerical optimization.

tation of the present study is that it only deals with the case of binary coatings. The authors are convinced that with a similar philosophy it is possible to derive optimal coating designs even in the case of layers made with three (possibly dissipative) materials, or even made with nano-layered [26] materials.

ACKNOWLEDGMENTS

This work has been partially supported by INFN through the projects Virgo and Virgo—ET. The author is grateful for the discussion and suggestions received from the Virgo Coating Research and Development Group and the Optics Working Group of the LIGO Scientific Collaboration. Special thanks to I.M. Pinto for his constant interest and encouragement in publishing this article.

[1] Virgo <http://www.virgo.infn.it>
[2] LIGO <http://www.ligo.caltech.edu>
[3] The LIGO Scientific Collaboration. Advanced LIGO. *Class. Quantum Gravity* **2015**, *32*, 074001.
[4] Acernese, F.; Agathos, M.; Agatsuma, K.; Aisa, D.; Allemandou, N.; Allocca, A.; Amarni, J.; Astone, P.; Balestri, G.; Ballardin, G.; et al. Advanced Virgo: A second-generation interferometric gravitational wave detector. *Class. Quantum Gravity* **2015**, *32*, 024001.
[5] The KAGRA Scientific Collaboration. Overview of KAGRA: Calibration, detector characterization, physical environmental monitors, and the geophysics interferometer. *Prog. Theor. Exp. Phys.* **2021**, *2021*, 05A102.
[6] Yam, W.; Gras, S.; Evans, M. Multimaterial coatings with reduced thermal noise. *Phys. Rev. D* **2015**, *91*, 042002.
[7] Steinlechner, J.; Martin, I.W.; Hough, J.; Kruger, C.; Rowan, S.; Schnabel, R. Thermal noise reduction and

absorption optimization via multimaterial coatings. *Phys. Rev. D* **2015**, *91*, 042001.
[8] Pierro, V.; Fiumara, V.; Chiadini, F.; Granata, V.; Durante, O.; Neilson, J.; Di Giorgio, C.; Fittipaldi, R.; Carapella, G.; Bobba, F.; et al. Ternary quarter wavelength coatings for gravitational wave detector mirrors: Design optimization via exhaustive search. *Phys. Rev. Res.* **2021**, *3*, 023172.
[9] Strutt, J.W. On the Reflection of Light from a Regularly Stratified Medium. *Proc. R. Soc. Lond. Ser. A Contain. Pap. A Math. Phys. Character* **1917**, *93*, 565–577.
[10] Abelès, F. La théorie générale des couches minces. *J. Phys. Radium* **1950**, *11*, 307–309.
[11] Born, M.; Wolf, E. *Principles of Optics: Electromagnetic Theory of Propagation, Interference and Diffraction of Light*, 7th ed.; Cambridge University Press: Cambridge, UK, 1999.

- [12] Orfanidis, S.J. *Electromagnetic Waves and Antennas*. Web Book. Available online: <https://www.ece.rutgers.edu/~orfanidi/ewa/> (accessed on 8 Dec. 2021).
- [13] Harry, G.; Bodiya, T.P.; DeSalvo R. *Optical Coatings and Thermal Noise in Precision Measurements*, 1st ed.; Cambridge University Press: Cambridge, UK, 2012.
- [14] Abernathy, M.R.; Liu, X.; Metcalf, T.H. An overview of research into low internal friction optical coatings by the gravitational wave detection community. *Mater. Res.* **2018**, *21*, e20170864.
- [15] Flaminio, R.; Franc, J.; Michel, C.; Morgado, N.; Pinard, L.; Sassolas, B. A study of coating mechanical and optical losses in view of reducing mirror thermal noise in gravitational wave detectors. *Class. Quantum Gravity* **2010**, *27*, 084030.
- [16] Pinard, L.; Sassolas, B.; Flaminio, R.; Forest, D.; Lacoudre, A.; Michel, C.; Montorio, J.L.; Morgado, N. Toward a new generation of low-loss mirrors for the advanced gravitational waves interferometers. *Opt. Lett.* **2011**, *36*, 1407–1409.
- [17] Pinard, L.; Michel, C.; Sassolas, B.; Balzarini, L.; Degallaix, J.; Dolique, V.; Flaminio, R.; Forest, D.; Granata, M.; Lagrange, B.; et al. Mirrors used in the LIGO interferometers for first detection of gravitational waves. *Appl. Opt.* **2017**, *56*, C11.
- [18] Pierro, V.; Fiumara, V.; Chiadini, F.; Bobba, F.; Carapella, G.; Di Giorgio, C.; Durante, O.; Fittipaldi, R.; Mejuto Villa, E.; Neilson, J.; et al. On the performance limits of coatings for gravitational wave detectors made of alternating layers of two materials. *Opt. Mater.* **2019**, *96*, 109269.
- [19] Herpin, A.; Cabannes, N.J. *Optique Electromagnétique—Calcul du Pouvoir Réflecteur dun Systeme Stratifie Quelconque*. *C. R. Acad. Sol.* **1947**, *225*, 182–183.
- [20] Agresti, J.; Castaldi, G.; DeSalvo, R.; Galdi, V.; Pierro, V.; Pinto, I.M. Optimized multilayer dielectric mirror coatings for gravitational wave interferometers. *Proc. SPIE* **2006**, *6286*, 628608.
- [21] Hadka, D.; Reed, P.M. Borg: An Auto-Adaptive Many-Objective Evolutionary Computing Framework. *Evol. Comput.* **2013**, *21*, 231–259.
- [22] Villar, A.E.; Black, E.D.; DeSalvo, R.; Libbrecht, K.G.; Michel, C.; Morgado, N.; Pinard, L.; Pinto, I.M.; Pierro, V.; Galdi, V.; et al. Measurement of thermal noise in multilayer coatings with optimized layer thickness. *Phys. Rev. D* **2010**, *81*, 122001.
- [23] Kondratiev, N.M.; Gurkovsky, A.G.; Gorodetsky, M.L. Thermal noise and coating optimization in multilayer dielectric mirrors. *Phys. Rev. D* **2011**, *84*, 022001.
- [24] Durante, O.; Di Giorgio, C.; Granata, V.; Neilson, J.; Fittipaldi, R.; Vecchione, A.; Carapella, G.; Chiadini, F.; DeSalvo, R.; Dinelli, F.; et al. Emergence and Evolution of Crystallization in TiO₂ Thin Films: A Structural and Morphological Study. *Nanomaterials* **2021**, *11*, 1409.
- [25] Țălu, Ș. *Micro and Nanoscale Characterization of Three Dimensional Surfaces. Basics and Applications*; Napoca Star Publishing House: Cluj-Napoca, Romania, 2015.
- [26] Pan, H.W.; Wang, S.J.; Kuo, L.; Chao, S.; Principe, M.; Pinto, I.M.; DeSalvo, R. Thickness-dependent crystallization on thermal anneal for titania/silica nm-layer composites deposited by ion beam sputter method. *Opt. Express* **2014**, *22*, 29847–29854.